Diego, CA, Aug. 1995.

[6]Braun, R. D., Powell, R. W., Engelund, W. C., Gnoffo, P. A., Weilmuenster, K. J., and Mitcheltree, R. A., "Six-Degree-of-Freedom Atmospheric Entry Analysis for the Mars Pathfinder Mission," AIAA Paper 95-0456, Jan. 1995.

[7]Boussalis, D., "Investigation of the Longitudinal Motion of Low-lift Entry Vehicles," Jet Propulsion Lab., TR EM 3456-96-002, California Inst. of Technology, Pasadena, CA, May 1996.

[8]Sofair, I., "Improved Method for Calculating Exact Geodetic Latitude and Altitude," *Journal of Guidance, Control, and Dynamics*, Vol. 20, No. 4, 1997, pp. 824–826.

[9]Tu, K.-Y., Munir, M., Mease, K., and Bayard, D., "Drag-Based Predictive Tracking Guidance for Mars Precision Landing," AIAA Paper 98-4573, Aug. 1998.

[10]Munir, M., "Entry Guidance Law for a Low Lift/Drag Mars Precision Landing," M.S. Thesis, Dept. of Mechanical and Aerospace Engineering, Univ. of California, Irvine, CA, 1997.

[11]Mease, K. D., and Kremer, J.-P., "Shuttle Entry Guidance Revisited Using Nonlinear Geometric Methods," *Journal of Guidance, Control, and Dynamics*, Vol. 17, No. 6, 1994, pp. 1350–1356.

C. A. Kluever
Associate Editor

Thermal and Structural Test Results for a Venus Deep-Atmosphere Instrument Enclosure

Jeffery L. Hall,* Paul D. MacNeal,† Moktar A. Salama,‡ Jack A. Jones,§ and Matthew Kuperus Heun¶
Jet Propulsion Laboratory, California Institute of Technology, Pasadena, California 91109-8099

Nomenclature

a, b = curve-fit constants
T = temperature, °C
T_{ref} = curve-fit reference temperature, °C
κ = thermal conductivity, W/m-K
κ_0 = thermal conductivity at reference temperature, W/m-K

Introduction

In situ exploration of the surface and deep atmosphere of Venus is impeded by an environment that is hostile to scientific instruments. Temperature, pressure, and corrosion protection must be provided to ensure survival of instruments and electronics for even short durations. Previous missions to Venus, namely the Soviet Venera landers and the U.S. Pioneer-Venus atmospheric probes, used a combination of titanium pressure vessels and thermal insulation for this purpose.[1,2] Recent work has investigated the possibility of using a balloon to deliver a small payload into the deep atmosphere of Venus for surface imaging and atmospheric investigations.[3–6] However, smaller payloads suffer from reduced volume-to-surface-area ratios and therefore heat up more quickly. This disadvantage has motivated the development of more efficient thermal insulation that retains the simplicity of design and operational robustness needed in the current era of smaller and cheaper space missions. The solution of using vacuum multilayer insulation (MLI) was originally suggested in the context of a novel Venus balloon mission concept capable of multiple descents into the hot lower atmosphere.[7] However, concerns about the efficiency of MLI on small spherical enclosures with multiple penetrations and the difficulty of ensuring the necessary high vacuum under Venus atmospheric pressure and temperature conditions led to a more robust alternative idea using fiberglass insulation with the void space filled with low thermal conductivity xenon gas. The present work investigated the performance of this xenon-filled fiberglass insulation in conjunction with a new, low thermal conductivity internal structure. A full-scale prototype was constructed and tested at simulated Venus surface temperature and pressure conditions. Also, a centrifuge test was performed to verify the ability of the structure to tolerate the expected deceleration load upon entry into the Venusian atmosphere. The details of the design and the test results are presented herein.

Prototype Design and Construction

The prototype design was guided by the mission specification of protecting 15 kg of payload at Venus surface conditions of 460°C and 9.2×10^6 Pa (92 atm) pressure. Optimal performance of the camera and other electronic components requires a near-Earthlike state, namely 10^5 Pa pressure and 20°C temperature. To meet the mission requirement of 1-h residence time near the surface of Venus, it was necessary to limit the heat flow to the payload to less than 100 W. The other key design driver was the need to survive typical deceleration loads when the probe enters the Venusian atmosphere from space. A nominal value of 250 g was selected for the prototype design based on the Pioneer-Venus experience[1,2] and current mission studies.[6]

The prototype is based on a concentric sphere design in which the payload is located within the inside sphere and thermal insulation is located in the annulus between the spheres. An expanded view of the enclosure is shown in Fig. 1, and a list of component masses is presented in Table 1. The spherical shape was selected because it results in the lightest structure per unit volume for withstanding external buckling loads, a fact that led to its use on the earlier Pioneer-Venus probes. As with those earlier probes, titanium alloy Ti-6Al-4V was selected for the outer sphere because of its excellent strength-to-weight ratio and its ability to tolerate the sulfuric acid found in the clouds of Venus. The nominal diameter is 38 cm, and the shell thickness is 0.38 cm, giving a diameter-to-thickness ratio of 100. Given an expected buckling failure mode, this shell has a computed 1.3 pressure safety factor at 460°C. For comparison, the Pioneer-Venus probes used a slightly less conservative design for which the diameter-to-thickness ratio ranged from 116 to 136 (Ref. 1).

The inside sphere is 30 cm in diameter with a wall thickness of 0.76 mm and is constructed from Type-304 stainless steel. The structure used to connect to the inside and outside spheres consists of three sets of rigid Ti-6Al-4V struts. The first is a single, thin-walled conical structure rigidly connected to the spheres at their south poles. This aperture cone is welded to the outer sphere and has a flange onto which the inside sphere is bolted. It is inside of this aperture cone that the camera window would be located in a fully functional probe. The second part is an array of six thin-walled Ti-6Al-4V struts arranged around the aperture cone. These six struts are welded to the outer sphere but have a nominal 0.5 mm gap at the inside sphere

Table 1 Mass list for prototype

Component	Mass, kg
Outer sphere	10.9
Inner sphere	4.2
Simulated payload	15.6
Fiberglass insulation	1.4
Miscellaneous	1.5
Total	33.6

Received 15 January 1999; revision received 6 August 1999; accepted for publication 20 August 1999.

*Staff Engineer, Advanced Thermal and Structural Technology Group, 4800 Oak Grove Drive. Senior Member AIAA.

†Senior Engineer, Instrument Structures and Dynamics Group, 4800 Oak Grove Drive. Member AIAA.

‡Principal Engineer, Instrument Structures and Dynamics Group, 4800 Oak Grove Drive. Associate Fellow AIAA.

§Principal Engineer, Advanced Thermal and Structural Technology Group, 4800 Oak Grove Drive. Senior Member AIAA.

¶Staff Engineer; currently Staff Engineer, Global Aerospace Corporation, P.O. Box 93305, Pasadena, CA 91109-3305.

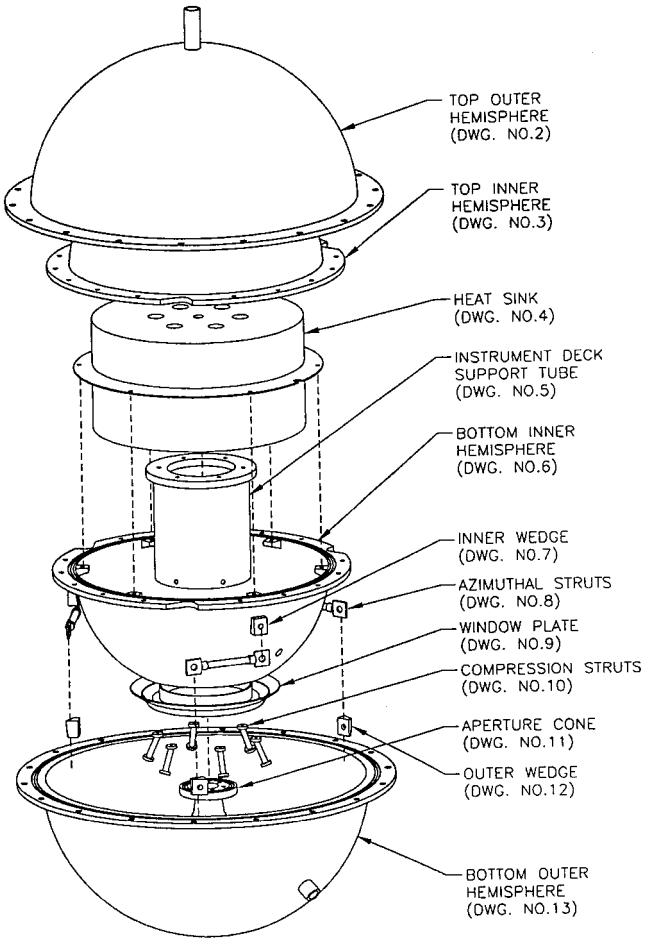

Fig. 1 Expanded view of prototype enclosure.

under 1 *g* loading. The concept is that when high deceleration loads are encountered the inside sphere will elastically deform and contact the six struts at which time they will share the structural load with the aperture cone. The aperture cone can therefore be designed with a thinner wall (0.5 mm) because it does not have to support all of the load by itself. The key advantage of this design is that the heat flow to the payload is minimized because not only does the Ti-6Al-4V alloy have an extremely low thermal conductivity (7.3 W/m-K at 20°C), but the six secondary struts do not contact the internal sphere at all during operation in the hot lower atmosphere. The third set of struts consists of three thin-walled Ti-6Al-4V tubes that are bolted near the equator of the spheres in a tangential direction. This provides side loading and torsional support during the crucial atmospheric entry phase.

The payload is simulated by a 15.6-kg aluminum block that is bolted to both an axial support tube and the flange of the inside sphere (Fig. 1). A small gap exists between the aluminum block and the inside sphere flange to ensure that the primary loading path is through the support tube and onward to the aperture cone and outside shell.

Thermal insulation is provided by microfiber felt composed of borosilicate glass fibers without any binder. Three sheets of thickness 1.3 cm and nominal density 96 kg/m^3 were used between the spheres. A total of three different insulating configurations were tested: air-filled insulation, 99.9% pure xenon-gas-filled insulation, and 99.9% xenon-gas-filled insulation plus four layers of two-sided, aluminized Mylar (MLI) placed between the insulation sheets and at either end.

Four Type-K thermocouples were cemented onto the outside of the enclosure to measure external temperatures. In addition, eight precision-integrated circuit temperature sensors were mounted inside, three to measure temperature on the inside sphere and five on the simulated payload. The eight internal sensors were multiplexed with an onboard microprocessor and transmitted through the two spheres via electrical feedthroughs. This signal was further multiplexed with the external thermocouple data and subsequently recorded on a portable computer with a nominal sampling time of 10 s.

Test Results and Discussion

The prototype successfully passed all three structural tests without damage. The first was a 25°C pressure test to 12 MPa (1740 psi) to simulate 1.3 times Venus surface pressure on the outside of the enclosure. This test was conducted in a remote facility consisting of a pressure vessel into which the prototype was placed. Nitrogen gas was injected between the pressure vessel and the prototype over a 40-min period until full pressure was achieved. The second test was a combined pressure and temperature test to 9.2 MPa and 460°C, which is the Venus surface condition. The remote facility from the first test was modified for this experiment to include electric heaters inside the pressure vessel and around the prototype. Pressure and temperature were simultaneously increased over a 75-min period until maximum conditions were attained. The third experiment was a centrifuge test at 250 *g*. For this test the enclosure was oriented such that the polar axis was aligned with the acceleration vector. Although the primary structure was undamaged during these tests, the electrical feedthrough in the outer shell was observed to leak under pressurization. This leak served to contaminate the xenon-gas-filled insulation and therefore yielded unreliable insulation performance data. The reason for the leak seemed to be inappropriate design rather than a manufacturing defect or faulty installation.

As a result of the feedthrough problem, the only reliable thermal data obtained were from three heating tests done in an oven at ambient pressure. Temperature data acquired from the internal sensors were combined with the known thermal capacity of the components to yield a total heat-flow through the insulation. The heat-flow data for all three tests is presented in Fig. 2. Note that the curve labeled "xenon-fiberglass-MLI" is offset in time on the graph so as to be more visible. The air-filled insulation clearly has a much higher heat flow than either of the two xenon cases (214 W vs 98 W at the maximum external temperature of 460°C). The two xenon cases show similar heating rates, suggesting that the addition of MLI did not have an appreciable effect on the insulating performance.

Quantification of the insulation performance corresponding to these tests depends on the details of the thermal model used to simulate the behavior. The model devised for this study was a one-dimensional unsteady nodal network composed of 11 nodes: 1 for the outside shell, 8 across the insulation, 1 for the inside shell, and 1 for the payload. In addition to node-to-node conduction across the insulation, the model included conduction along the outer to inner shell connecting struts based on the known strut geometry and thermal conductivity of Ti-6Al-4V alloy. The unknown in the analysis was the effective thermal conductivity κ of air and xenon-filled

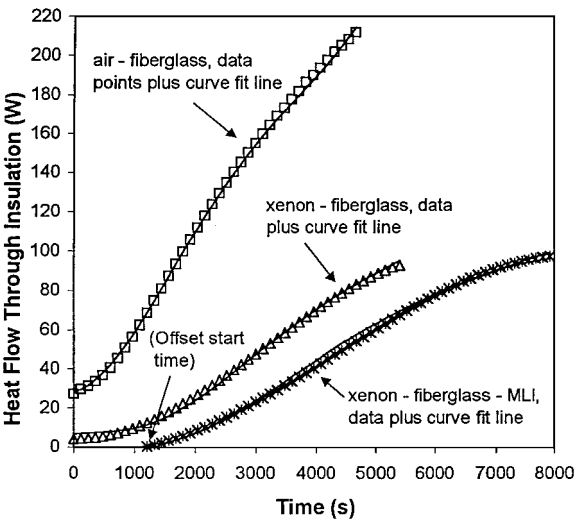

Fig. 2 Heating data for prototype tests.

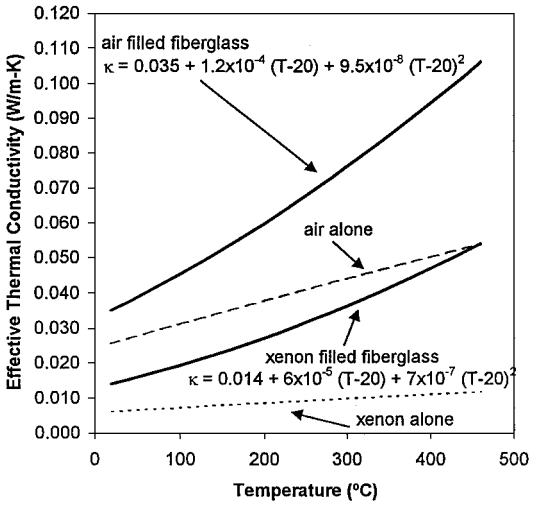

Fig. 3 Effective thermal conductivity vs temperature.

fiberglass insulation as a function of temperature. An equation of the form

$$k(T) = k_0 + a(T - T_0) + b(T - T_0)^2 \qquad (1)$$

was assumed for each gas, where T_0 was defined to be 20°C and the constants κ_0, a, and b determined by fitting the model output to the data of Fig. 2. As can be seen, reasonably good agreement was obtained by curve fitting the data in this fashion. The resultant $\kappa(T)$ functions are plotted and listed in Fig. 3. The xenon-filled fiberglass is seen to have roughly one-third the conductivity of air-filled fiberglass at room temperature and half the conductivity at 460°C. At 20°C both insulations are 0.008 W/m-K more conductive than their parent gases alone (Fig. 3), suggesting that the fiberglass itself contributes this amount to the overall conductivity. The fact that the gas-filled fiberglass conductivities increase with temperature more quickly than the parent gases alone is an indication of substantial radiative heat transfer at the higher temperatures. At 460°C the radiative component, as estimated by subtracting out the parent gas and fiberglass conductive components, is 0.034 W/m-K for xenon-filled fiberglass (63%) and 0.044 W/m-K (41%) for air-filled fiberglass. Note that both xenon heating curves in Fig. 3 have been fitted by the same $\kappa(T)$ function, demonstrating that the addition of aluminized Mylar did not reduce the radiative heat transfer.

Finally, the measured heat flux to the simulated payload was 84 W for the xenon-filled fiberglass and 189 W for the air-filled fiberglass at the simulated Venus surface temperature of 460°C. The xenon value therefore satisfies the original enclosure design target of being less than 100 W. A further 26 W for the xenon case and 46 W for the air case accumulate in the inner shell at this maximum 460°C external temperature to yield a total outside to inside heat flow of 110 and 226 W, respectively. Only 12 W of these totals is caused by conduction through the titanium struts.

Conclusions

Experimental data and analysis were presented for a prototype of a small, lightweight protective instrument enclosure for use near the surface of Venus. The novel features of the device included a concentric sphere geometry, xenon-gas-filled fiberglass insulation, and a low thermal conductance internal structure. Integrity of the overall structure under simulated Venus surface pressure and atmospheric entry deceleration loads was successfully demonstrated. Heating measurements yielded an effective thermal conductivity for the prototype for both xenon- and air-filled fiberglass insulation. For xenon this conductivity ranged from 0.014 W/m-K at 20°C to 0.054 W/m-K at 460°C. The net heat flow at 460°C to the simulated payload through xenon-filled insulation was 84 W, well within the required mission design goal of 100 W.

Acknowledgments

This research was carried out at the Jet Propulsion Laboratory, California Institute of Technology, under contract sponsored by NASA. Funding for this research was provided by the JPL Director's Research and Development Fund. The authors acknowledge and thank James Cutts of JPL's Special Project's Office for his guidance and Patrick O'Brien, Shannon Jackson, José Rivera, and Scott Leland, also of JPL, for their valuable technical assistance. National Technical Systems of Saugus, California, provided the high pressure and centrifuge test facilities for this project.

References

[1]Hughes Aircraft Company, *Pioneer Venus Case Study in Spacecraft Design*, AIAA, New York, 1979.

[2]Colin, L., and Hall, C. F., "The Pioneer Venus Program," *Space Science Reviews*, Vol. 20, D. Reidel, Dordrecht, The Netherlands, 1977, pp. 283–306.

[3]Jones, J. A., "Reversible Fluid Balloon Altitude Control Concepts," AIAA Paper 95-1621, May 1995.

[4]DiCicco, A. G., Nock, K. T., and Powell, G. E., "Balloon Experiment at Venus (BEV)," AIAA Paper 95-1633, May 1995.

[5]Lorenz, R. D., "Design Considerations for Venus Microprobes," *Journal of Spacecraft and Rockets*, Vol. 35, No. 2, 1998, pp. 228–230.

[6]Cutts, J. A., Kerzhanovich, V., Balaram, J., Campbell, B., Gershman, R., Greeley, R., Hall, J. L., Cameron, J., Klaasen, K., and Hansen, D. M., "Venus Aerobot Multisonde Mission," AIAA Paper 99-3857, June 1999.

[7]Heun, M. K., Jones, J. A., and Hall, J. L., "Gondola Design For Venus Deep Atmosphere Aerobot Operations," AIAA Paper 98-0897, Jan. 1998.

R. B. Malla
Associate Editor

Propulsive Efficiency of Hypersonic External Burning

G. E. Dorrington*
University of London,
London, England E1 4NS, United Kingdom

Introduction

THE idea of using external burning for propulsion in hypersonic flowfields has been proposed for various aerospace applications. Cuadra and Arthur,[1] for example, suggest external burning might be used for propulsive orbit plane change maneuvers. In the 1960s and 1970s, however, most interest in external burning appears to have been directed toward hypersonic cruise vehicles. In particular, Küchemann[2] discusses propulsive lifting bodies in support of his global transportation philosophy. Here Küchemann draws upon the theoretical studies of Oswatitsch[3] and Zierep[4,5] who derive linearized expressions for the propulsive efficiency of two-dimensional bodies with external burning in supersonic and hypersonic flows, respectively.

This Note briefly reintroduces the just-mentioned theoretical studies and sets out a simple isobaric slice analysis (ISA) method to obtain Oswatitsch's expression in a direct manner. The method is then extended to obtain an alternative approximation for propulsive efficiency in hypersonic flows, which sets a lower bound than indicated by Zierep. The approach used is believed to be original, although it bears some resemblance to an analysis by Gazley.[6]

Like the aforementioned works,[3–6] the ISA method assumes perfect gas relations. Real gas effects and viscous flow effects are ignored, and the simple analytical approximations developed here may

Received 2 December 1998; revision received 30 July 1999; accepted for publication 30 July 1999.

*Lecturer in Aerospace Design, Department of Engineering, Queen Mary and Westfield College.